Controlling Thermal Expansion: A Metal-Organic Frameworks Route

Balestra, S.R.G.; Bueno-Perez, R.; Hamad, S.; Dubbeldam, D.; Ruiz-Salvador, A.R.; Calero, S.

DOI
10.1021/acs.chemmater.6b03457

Publication date
2016

Document Version
Final published version

Published in
Chemistry of Materials

CHEMISTRY OF MATERIALS

Article

pubs.acs.org/cm

Controlling Thermal Expansion: A Metal–Organic Frameworks Route

Salvador R. G. Balestra,[†] Rocio Bueno-Perez,[†] Said Hamad,[†] David Dubbeldam,*[,‡] A. Rabdel Ruiz-Salvador,*[,†] and Sofia Calero*[,†]

[†]Department of Physical, Chemical, and Natural Systems, Universidad Pablo de Olavide, Ctra. Utrera, km 1, 41013 Seville, Spain

[‡]Van't Hoff Institute for Molecular Sciences, University of Amsterdam, Science Park 904, 1098 XH Amsterdam, The Netherlands

Supporting Information

ABSTRACT: Controlling thermal expansion is an important, not yet resolved, and challenging problem in materials research. A conceptual design is introduced here, for the first time, for the use of metal–organic frameworks (MOFs) as platforms for controlling thermal expansion devices that can operate in the negative, zero, and positive expansion regimes. A detailed computer simulation study, based on molecular dynamics, is presented to support the targeted application. MOF-5 has been selected as model material, along with three molecules of similar size and known differences in terms of the nature of host–guest interactions. It has been shown that adsorbate molecules can control, in a colligative way, the thermal expansion of the solid, so that changing the adsorbate molecules induces the solid to display positive, zero, or negative thermal expansion. We analyze in depth the distortion mechanisms, beyond the ligand metal junction, to cover the ligand distortions, and the energetic and entropic effect on the thermo-structural behavior. We provide an unprecedented atomistic insight on the effect of adsorbates on the thermal expansion of MOFs as a basic tool toward controlling the thermal expansion.

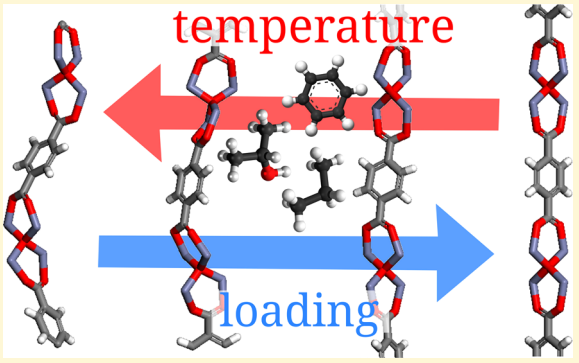

INTRODUCTION

Thermal expansion (TE) mismatch is at the core of common mechanical failures in a wide range of systems.[1−4] This is an intriguing problem that needs to be solved for the development of new applications in advanced industries such as aerospace and microelectronics. To overcome this problem, it is desirable to have materials with controlled thermal expansion (CTE), a topic that has been of high interest for decades.[1,3,5,6] Currently, the most frequently used choice is composite materials, whose TE can be controlled by adjusting the amount of components having positive (PTE) and negative thermal expansion (NTE) in such a way that the overall behavior fits the targeted necessities.[5] Composite materials, however, have a high concentration of interfaces, which are weak points, not only from a mechanical, but also from a chemical point of view, mainly at medium and high temperatures.[7,8] There is therefore a great interest in finding systems where the control of the thermal expansion can be achieved without having to resort to composite materials.

Recently, Evans and co-workers successfully prepared cubic $Zr_{1-x}Sn_xMo_2O_8$ solids and found an unprecedented level of chemical control of the thermal expansion (negative, zero, and positive) in a single phase over a very wide range of temperatures.[6] They started from the known fact that oxide frameworks, such as cubic ZrW_2O_8, show NTE,[9] while the analogous $SnMo_2O_8$ is unique in showing PTE. Shortly after, Carey et al. studied the TE of dehydrated Li-, Na-, K-, Rb-, Cs-, and Ag- exchanged zeolite A and their purely siliceous analogue, ITQ-29.[10] They found that, in dehydrated state, NTE dominates in most cases, except for Li- and Ag-forms, which show a small PTE. On the other hand, PTE is observed in the presence of water. These approaches stimulate the search for materials that can be easily prepared and readily tuned to obtain ad hoc thermal expansion coefficients. Since a number of metal–organic frameworks (MOFs) are known to show NTE,[11−13] it is interesting to investigate whether MOFs can be used to develop systems with controlled thermal expansion. This is also stimulated by the recent study of Yot and co-workers, which shows that MOFs can be used as shock absorber.[14] In this context, exploitation of the mechanical properties of MOFs emerges as a fascinating new branch in MOFs applications horizon.[15]

Following the surprising TE behavior of some zeolites and inorganic framework solids, such as oxides and cyanides, a number of experimental and theoretical studies have been directed to study the thermostructural behavior of MOFs. Dubbeldam et al. predicted exceptional NTE in MOF-5 by using molecular simulations,[16] which achieved good agreement with the experimental behavior of the material loaded with CO_2, N_2, and Ar,[17] results that were later validated experimentally for the empty framework.[18] Omary and co-workers found a MOF that undergoes PTE when desolvated,

Received: August 18, 2016
Revised: October 24, 2016
Published: October 25, 2016

DOI: 10.1021/acs.chemmater.6b03457
Chem. Mater. 2016, 28, 8296−8304

but it contracts in the presence of N_2 at temperatures below 119 K, while it expands at higher temperatures.[19] Joo et al. predicted a cell volume contraction due to van der Waals interactions of guest H_2 molecules in MOF-5.[20] Lock et al. found experimentally that the NTE observed in MOF-5 decreases with the amount of loaded helium.[12] In addition, cell contraction in the breathing MOF MIL-53, induced by attractive host−guest interactions, has been identified.[21,22] In addition, Grobler et al.[23] observed that the extent of PTE in an anisotropic MOF can be tuned by the adsorption of molecules, and that the size of the molecules is correlated with the induced change of the CTEs. All these findings point to the validity of the hypothesis that MOFs can be tuned to be materials with tailored CTE coefficients. In this theoretical study, we show that by controlling the nature and amount of adsorbed molecules in a MOF, the TE coefficient can be finely tuned to display a desired behavior (PTE, NET, or ZET, i.e., Zero TE). Note that large, deformable MOFs, like MIL-53,[24] or soft coordination polymers[25] are not likely to be useful CTE materials, as their volume changes usually exceed the required adjustment of the TE-induced size mismatch.

As the material of study, we have selected MOF-5,[26] considering that not only is it an archetypal MOF, but also most importantly that molecular simulation methods perform very well in modeling its thermal behavior, including the NTE.[16] The adsorption of polar molecules in MOF-5,[27] is known to occur in the proximity of the metal oxoclusters. Since the formation of water clusters in this material provokes chemical instability,[27] we have chosen an alcohol molecule, isopropanol (IPA), to study the influence of polar adsorbate−metal oxocluster interactions in its thermal behavior. Similarly, but for comparative purposes, we have also studied the adsorption of benzene (BEN), to observe the behavior associated with nonpolar adsorbate−ligand interactions, as the role of the ligands in adsorption in MOF-5 has been identified to be of the same order than that of the oxocluster.[28] Experimental results have shown that the ligands in MOF-5 also act as adsorption sites.[17] Other authors, by using molecular simulation, found similar conclusions with regard to the presence of an adsorption site next to the ligands.[29,30] A detailed discussion of the effect of metals and ligands on the adsorption properties of MOFs can be found in a review by Andirova et al.[31] In the present case, since benzene, as an adsorbate, can interact with the benzene ring of the ligand, via $\pi-\pi$ interactions,[32] it is interesting to consider also a linear alkane. We have chosen propane (PRO) as nonpolar adsorbate with no particular interaction with the MOF. The overall behavior of MOF-5, when guest molecules are adsorbed, is expected to be the result of a balance between three factors, namely (a) the attractive host−guest interactions, (b) the vibrational modes of the MOF structure (by taking into account that they are likely to be affected by the adsorbates), and (c) the repulsive contributions from adsorbate−framework collisions, which are more relevant at higher temperatures. We note that MOF-5 collapses at relatively low external pressures,[33] which precludes its use at high mechanical stresses. Nevertheless, this system has other advantages. The material is an appropriate model system, considering the available experimental and theoretical literature on its thermal behavior, and on the other hand, it can be used for controlling TE in small devices, such as those required in microelectronics.

CONCEPTUAL DESIGN, METHODS, AND COMPUTATIONAL DETAILS

In this work, we introduce a new concept in MOFs applications: their use as materials for controlling thermal expansion in the three regimes, namely negative, zero, and positive. As described in the Introduction, there is a large amount of published studies accounting for interesting thermo-structural behaviors of MOFs, including changes of the thermal expansion with adsorbed molecules, which support the devised application. Our approach consists in the design of coatings made by MOFs, which are loaded with a certain amount of adsorbate molecules. These MOFs can have a desired, specific thermal expansion that covers the entire range of behaviors, that is, negative, zero, and positive expansions. It is well-known that a number of MOFs suffer damage upon desolvation, which can even lead to loss of crystallinity and structural collapse or amorphization.[34] The presence of guest molecules in a MOF can enhance its mechanical resistance against framework collapse.[35] Therefore, a careful selection of the MOF and the adsorbate molecules is essential. Nowadays, there are several robust MOFs that have been proven to withstand cycles of solvation and desolvation, such as those studied by Janiak et al., on MIL-101,[36] and Begum et al.[37] Chemical stabilization of certain MOFs, which are known to collapse otherwise, can be achieved by applying solvent exchange to remove the pristine molecules in the pores resulting from the synthetic procedure. Such molecules might exert large capillary forces on desolvation, which lead to collapse, but an exchange with weak-interacting solvents can prevent it.[38] We have paid attention to the known fact that the equilibrium loading of adsorbate molecules in a porous material depends on temperature, pressure, and the nature of the molecules. In this regard, since the planned application involves variations of temperature, and implicitly also of external pressure, the device used for controlling thermal expansion must be operated without molecular exchange with the environment.

Simulations were performed with the RASPA code.[39] The isosteric heats of adsorption of the guest molecules were computed after 500 000 sampling steps using the fluctuation formula.[40] Adsorbate−adsorbent interactions were modeled with Lennard-Jones (LJ) pairwise interatomic potentials plus Coulomb interactions. The values of the LJ parameters were calculated through Lorentz−Berthelot mixing rules, for which the force field parameters of the atom of the MOF were taken from the UFF force field,[41] and those of isopropanol, propane, and benzene molecules were taken from the OPLS-AA force field.[42,43] The LJ interactions were computed in the real space, with a cutoff of 12 Å, while the Coulomb interactions were handled using the Ewald summation method.[44,45] The atomic charges used for the molecules were then taken from the selected force field, and those of the MOF atoms were taken from Dubbeldam et al.[16] The overall thermostructural behavior is expected to depend, particularly at high adsorbate loadings, on the adsorbate−adsorbate interactions as well as on the framework properties and framework−adsorbate interactions. Therefore, we did not only pay careful attention to the force field used for the framework, but also for the adsorbates. The force fields employed to model guest−guest interactions have been proven to model accurately the liquid phases of the compounds[46−48] so that we can rely on their validity for modeling the dense phases within the pores.

Monte Carlo (MC) simulations in the Canonical (NVT) ensemble were conducted initially with one adsorbate molecule to compute average occupancy profiles of each adsorbate. This was used as a tool for localizing the adsorption sites and to calculate the binding energies of the adsorbates on the preferential sites. The maximum loading capacities were extracted from the saturation of the adsorption isotherms computed in the Gran Canonical (μVT) ensemble. To insert successfully the molecules in the system, the Configurational Bias Monte Carlo (CBMC) technique was used.[49] NVT MC simulations were conducted with 20, 40, 60, 80, and 100% saturation of adsorbate molecules as starting configurations for the subsequent molecular dynamics (MD) simulations. MC simulations were run with 80 000 and 1 000 000 equilibration and production steps, respectively.

DOI: 10.1021/acs.chemmater.6b03457
Chem. Mater. 2016, 28, 8296−8304

MD simulations were performed in the isothermal−isobaric ensemble (NPT), with isotropic cell fluctuations, using the fully flexible force field reported by Dubbeldam et al.[16] for the description of the thermostructural properties of MOF-5, with and without adsorbate molecules. The integration of the equations of motion that generate the NPT ensemble was performed following the scheme of Martyna et al.[50,51] A short time step, of 0.5 fs, was used to avoid the generation of abnormally large interatomic forces that might eventually induce the partial collapse of the framework. A total of 200 000 steps (100 ps) were used for the equilibration of the systems and 10 000 000 steps (5 ns) for the production run. The adsorbate−adsorbent interactions were computed in the same way as used for the computation of the heats of adsorption. The structural data, acquired from the MD simulations, were analyzed with a homemade code, explicitly written for this purpose, which allowed partitioning of the cell length deformations among the different geometrical units that compose the material.

RESULTS AND DISCUSSION

We first present some introductory results that are useful, on the one hand for validating the theoretical methods, and on the other hand to describe the host−guest interactions between MOF-5 and the selected guest molecules. The closest available experimental results with which we can compare, regarding the variation of the thermal expansion of MOF-5 produced by changes in the amount of adsorbed molecules, are those reported by Lock et al.[12] They employed helium flows at different rates to vary the amount of adsorbate molecules. We have therefore simulated this system to show the reliability of our computer simulation protocol, though it is worth mentioning that only qualitative comparisons can be established since an accurate, quantitative estimation of the resident helium atoms inside the MOF in gas-flow operando experimental conditions is not possible. To obtain the best possible estimate, we calculate the number of helium atoms in the GCMC simulations at the pressures used to set the helium fluxes in the experiments of Lock et al.[12] In Figure 1, we plot

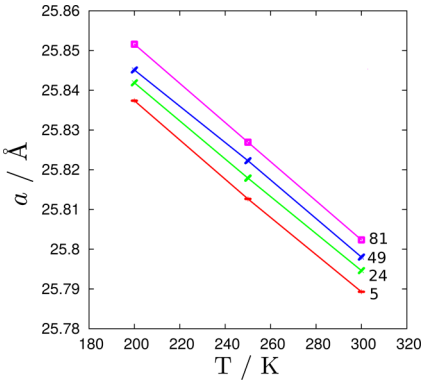

Figure 1. Variation of the cell parameter, *a*, of MOF-5 with temperature, *T*. The MOF was loaded with 5, 24, 49, and 81 helium molecules per unit cell (red, green, blue, and pink lines, respectively).

the dependence of the cell volume of MOF-5 with temperature, for different amounts of helium atoms (below 10% of saturation capacity). It shows reasonable agreement with the experimental results,[12] since the correct NTE behavior is present, while there is an increase of cell parameters as the number adsorbed helium molecules increases. We did not get a decreasing behavior of the NTE coefficient as the number of guest molecules increases, because the number of flowing helium atoms per unit cell in the experiments is likely to be much higher than the value we obtain for the equilibrium calculation (ca. 10% of saturation) through GCMC. With these results in mind, we will now show that by increasing the number of adsorbate molecules, the NTE coefficient can indeed be tuned.

Using the selected probe molecules, we will provide a rationalization off the behavior found in Figure 1. As stated earlier, the nature and strength of the interactions of the guest molecules with the material are expected to play an important role in its overall thermostructural behavior. Accordingly, MC simulations were used to study the adsorbate−adsorbent interactions for the selected three molecules. The heats of adsorption, adsorption entropies, Henry coefficients, and binding energies are reported in Table 1. The strength of the host−guest interactions, as expected, increases with the number of non-H atoms. In general, single adsorbate molecules are preferentially located near the zinc atom of the oxocluster, in a corner also delimited by the adjacent atoms of the three benzene rings (Figure 2). In the MOF-5 structure, there are two types of cages, big and small, with different degrees of rotation of the benzene rings in the linker. Our results show that the three guest molecules studied occupy mainly the big cages in first place. The distribution of molecules around the oxocluster is different between benzene, which spreads up to the benzene rings in the linkers, and isopropanol and propane, which are rather concentrated around the oxocluster. Likewise, the different nature of the adsorption of isopropanol and propane is evidenced by the wider area that the latter occupies around the oxocluster. This is also supported by the different behavior found in the adsorption isotherms (Figure S2).

Along with the occupation profiles, the heats of adsorption and binding energies reveal that dispersive van der Waals interactions represent an important contribution to host−guest interactions. It is also noticeable that the stronger electrostatic interaction of isopropanol increases its binding energy. In the case of benzene, the $\pi-\pi$ interactions are responsible for the high binding energy. Nevertheless, the large porosity and heterogeneity of binding sites of this material lead to a much lower average interaction strength. This is also reflected in the entropy and Henry coefficients, and from a structural point of view, this is revealed by slight changes of the atomic density near the oxocluster: isopropanol is more concentrated than propane at the corner of the oxocluster, and benzene is also likely to occupy an intermediate position between the oxocluster and the benzene ring in the linker. We noted that at high loading conditions the sites in the small cages are also are occupied by guest molecules (Figure S1).

The adsorption saturation capacities in MOF-5, as calculated by GCMC simulations at high pressure, are 86, 98, and 105 molecules per unit cell for benzene, isopropanol, and propane, respectively. As expected when we selected the molecules with similar molecular sizes, differences in the number of molecules do not exceed 20%. Note that a cell volume change of the MOF should lead to a variation in the number of molecules in saturation conditions. However, the variation of volume is tiny, compared with the total volume, and consequently the largest deviation in the number of molecules is less than 3.2%. We note that the comparison of the computed saturation capacity with experiments is only possible with benzene;[52,53] as for the other two molecules, there are not available published data. The difference between the two experimental values available differs by 12.66% (8.95 mol/kg and 10.24 mol/kg, in the studies of Shim et al.[53] and Eddaoudi et al.,[52] respectively), which is not surprising considering that the presence of defect and residual

DOI: 10.1021/acs.chemmater.6b03457
Chem. Mater. 2016, 28, 8296−8304

Table 1. Calculated Isosteric Heats of Adsorption, (ΔH), Adsorption Entropies, (ΔS), Binding Energies, (ΔU), Binding Energies at Minimum Energy Configuration, (ΔU^*), and Henry Coefficients, (K_H), of Benzene, Isopropanol, and Propane in MOF-5 at 300 and 500 K

	T (K)	ΔH (kJ/mol)	ΔU (kJ/mol)	ΔU^* (kJ/mol)	$T\Delta S$ (kJ/mol)	K_H (mol/kg/Pa)
benzene	300	−32.34	−29.85	−40.80	−10.87	1.381×10^{-3}
	500	−28.16	−24		−10.35	1.082×10^{-5}
iso-propanol	300	−27.16	−24.66	−41.84	−10.26	2.173×10^{-4}
	500	−22.52	−18.36		−8.66	4.18×10^{-6}
propane	300	−21.41	−18.91	−31.11	−7.45	6.7×10^{-5}
	500	−19.46	−15.3		−7.59	2.587×10^{-6}

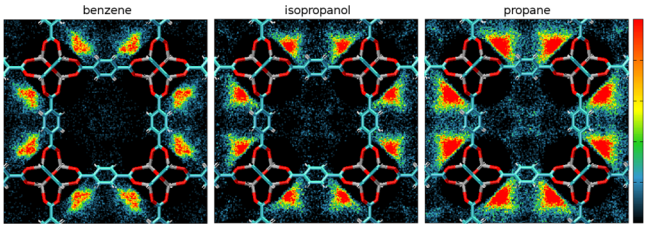

Figure 2. Average occupation profiles of the center of mass of the adsorbate molecules (benzene, isopropanol, and propane) in an xy-view. The cages located at the center and the corners of each snapshot correspond to the small cage. The framework atoms are superimposed to get a better understanding of the density profiles. The color code of the framework atoms is carbon, blue; oxygen, red; hydrogen, white; zinc, gray.

dimethylformamide from the synthesis might alter the otherwise ideal adsorption capacity. It is also relevant that both experiments are conducted only to relatively low pressure values (less than 10 kPa). Our simulations are conducted in defect-free, completely desolvated frameworks, and the computed loading value at the pressure where adsorption saturation is observed (ca. 1 kPa) is within 15% (11.96 mol/kg) of the experimental data, which is a reasonably good agreement. In addition, as an important point for practical applications, it is useful to see that 98% of adsorption saturation is reached at experimentally accessible pressures (Figure S2).

Once the basic introductory data have been presented, we will carry out the analysis of the thermal expansion. The wide range of thermal expansion behaviors of MOF-5 loaded with benzene (BEN-MOF-5), isopropanol (IPA-MOF-5), and propane (PRO-MOF-5) is displayed in Figure 3. MOF-5 has a cubic space group, and therefore, we only plot the cell volume. Three regimes are clearly observed: NTE, PTE, and ZTE. We found that the simulated thermal behavior of the bare framework is in fair agreement with the experimental data. This was also observed in a previous work.[16] It is worth noting that, while the variation of the cell parameter of the mixed oxide solution of Evans and co-workers is of the order of 0.5%, in this system we find a larger variation, of 2.7%, that is, a range of variation five-times larger.

A remarkable conclusion that can be drawn from Figure 3 is that the system shows a colligative behavior, that is the qualitative behavior of the material does not depend on the choice of the adsorbed molecule. This is somehow surprising, as we noted that the interaction energies of the molecules with the framework as single entities (Table 1) are different. Nevertheless, it is clear that the nature of the molecules allows a fine-tuning of the volume variation, but the overall behavior is qualitatively the same for the three types of adsorbed molecules. The appearance of colligative behavior has not yet been reported in MOFs or coordination polymers.

The key point in controlling the thermal dependence of the cell volume is the degree of guest loading. As shown in Figure 3, below 40% the NTE regime is observed, and PTE appears above 80%, while ZTE appears between these two values. To rationalize this interesting behavior, it is instructive to focus first at very low temperatures. In this situation, the influence of the attractive host−guest interactions on the structure contraction is large. This is evidenced by cell volume values below saturation at 200 K that are lower than that of the bare structure. For instance, benzene molecules are attracted by the aromatic rings of the linkers, as shown in the snapshot of MOF-5 at 300 K, and a benzene loading of 20% (Figure 4b). In a second stage, it is interesting to pay attention to the behavior at loadings close to saturation, where the guest-induced molecular pressure on the framework is dominant, which leads to cell volume increases, and the display of the PTE regime. As anticipated earlier, it is apparent that two effects compete in directing the thermal behavior: host−guest attraction and

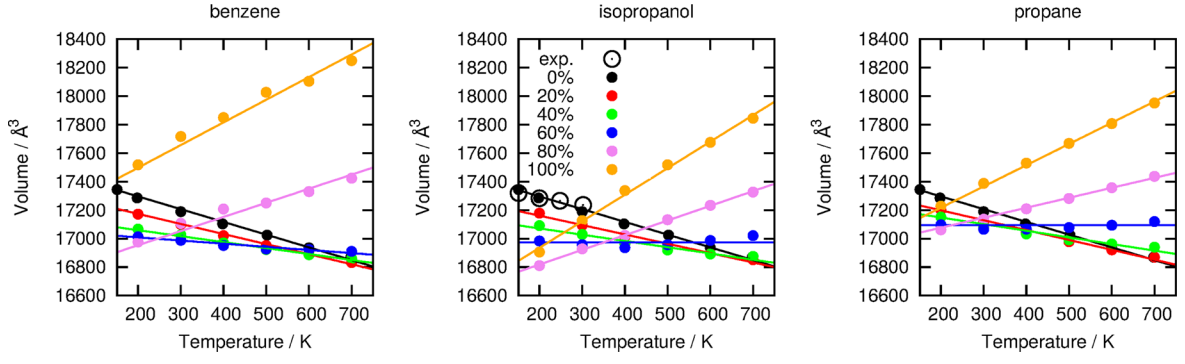

Figure 3. Cell volume as a function of temperature for several loadings (in % of saturation) of benzene, isopropanol, and propane. Experimental data are taken from refs 26 and 54. Solid lines represent linear regressions ($r^2 > 0.9$). The color code is the same for the three figures.

DOI: 10.1021/acs.chemmater.6b03457
Chem. Mater. 2016, 28, 8296−8304

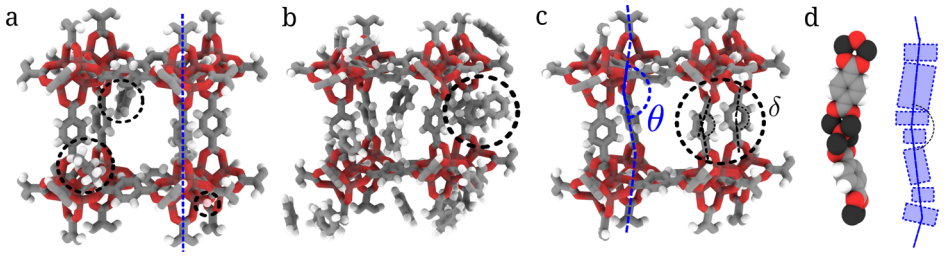

Figure 4. (a) Structure of idealized, undistorted MOF-5 with the guest molecules in their corresponding binding sites. (b) Snapshot of the structure with 20% of saturation of benzene. We show benzene molecules interacting with a benzene molecule of the linker via $\pi-\pi$ interactions. (c) Distorted structure. Dashed blue lines represent a schematic view of the string of atoms crossing the cell, with different degrees of distortions θ, and δ represents small distortions in the BDC linker. (d, left) String of atoms crossing the cell. (d, right) Schematic view of the line distorted string.

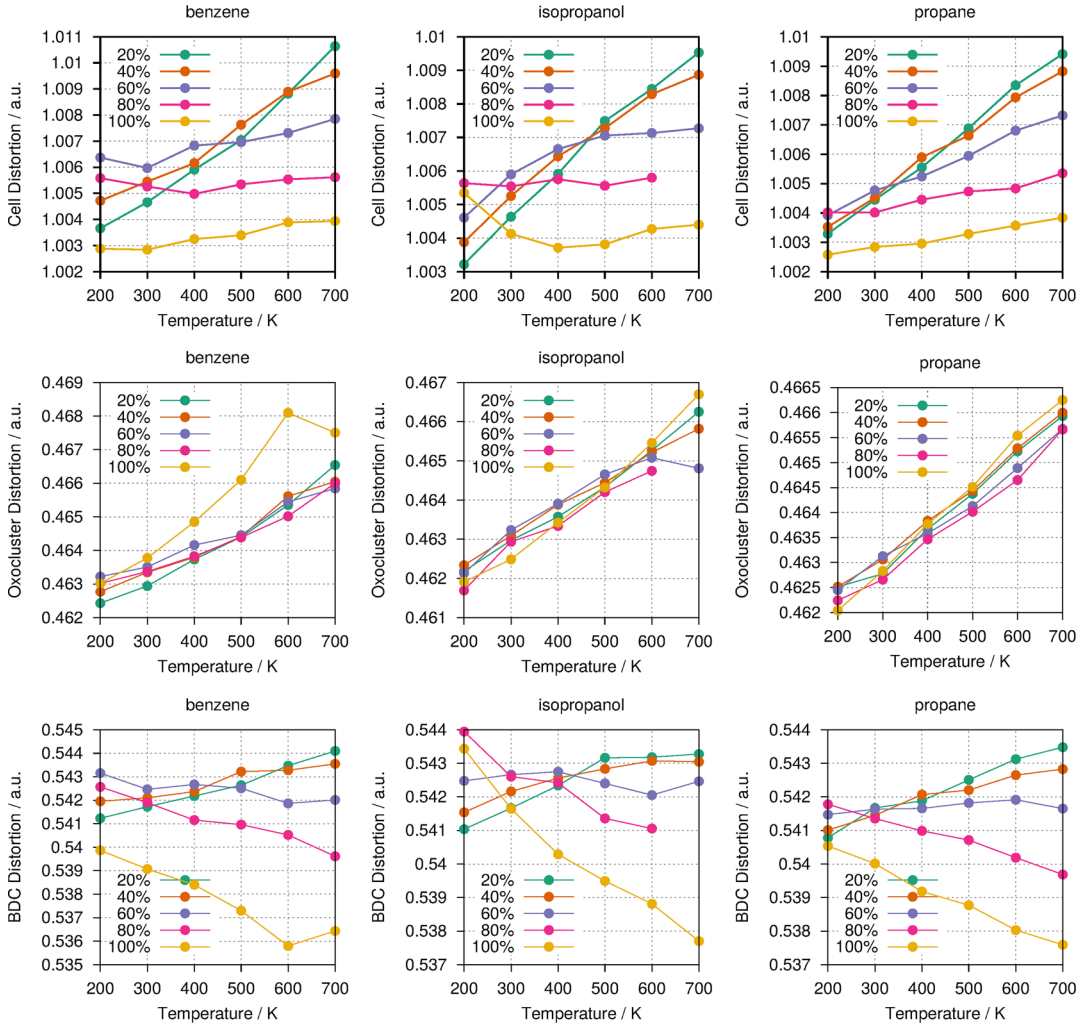

Figure 5. Variation, as a function of temperature of (top) the cell distortion, (middle) the oxocluster distortion, and (bottom) benzenedicarboxylate (BDC) distortion, for benzene, isopropanol, and propane. The distortions are defined in the text and in the Supporting Information (Equation S1). Note that oxocluster plus BDC distortion sum is about 1.

guest−induced pressure. The calculated TE coefficients systematically increase with a rise of the number of adsorbate molecules present in the structure. For the three molecules, at loadings of 20% of saturation, the TE coefficients are around -40×10^{-6} K^{-1}, they are nearly zero at 60% loading, and the saturation values are 80×10^{-6} K^{-1} for BEN and PRO and 107×10^{-6} K^{-1} for IPA. Details are given in the Supporting Information (Figure S3 and Table S2).

To obtain further insights into the thermal behavior of the system, we analyze the relationship between molecular interactions, local deformations, and TE. From previous work, it is known that the NTE observed in MOF-5 is not associated with a concerted rotation of the oxocluster,[16] as it would be expected from the behavior in inorganic framework materials.[55−57] Although several studies have addressed this point,[12,18,58−60] the question remains still open, particularly when guest molecules are present. Here, we perform a real space analysis of the system to get a better picture of the effect of the adsorbates over the structural behavior. As expected, in all cases, the bonds of the solid elongate as temperature

DOI: 10.1021/acs.chemmater.6b03457
Chem. Mater. 2016, 28, 8296−8304

increases (Figure S5). Therefore, a rationalization of the peculiar TE observed should be provided by the analysis of the collective behavior.

By using lattice dynamics DFT calculations, Zhou et al. found that a number of low energy modes are associated with deformation of BDC ligands.[18] They did not identify them as a likely source of the observed NTE behavior, but they considered the BDC ligands as rigid units, as well as the oxocluster, and only linked the NTE with the junction flexibility. Further understanding was obtained by combining diffraction studies and cluster model DFT calculations of the empty framework MOF-5.[59] They suggested that the motions associated with low energy modes, which are responsible of NTE, are not only linked to the flexibility of connecting junctions, but also to intraunit (ligand and oxocluster) motions.[59] Since our study comprises periodic MD simulations, which for structural dynamics studies is benefited by the absence of symmetry constrains within the unit cell,[61] here we focus on both the junction units and intraunit deformations as well as on their relation to the observed complex thermo-structural behavior. It is worth noting that this analysis can provide a knowledge that will be useful for achieving control of the thermal expansion.

The structure of MOF-5 can be described as a 3-D grid structure, built up by strings that cross the cell, parallel to the axes (dashed blue line, in Figure 4a). There is a degree of flexibility along the rods composing the strings, and it is easy to visualize that the further away the strings of atoms are from a perfect line (a schematic view in Figure 4c,d), the shorter will be the corresponding cell axis. The rods represent the segments between the midpoints of the pair of oxygen atoms of each carboxylate group and are depicted by blue bars in the schematic view of Figure 4, panel d. More details are given in the Supporting Information (Figure S4).

To quantify the structural changes, we have plotted the ratio between the sum of the length of four rods and the length of the cell axis parallel to each line. We called this value "cell distortion", and it is displayed in Figure 5 (top) and in Equation S1. Two different regimes are found: an almost linear increase, at loadings below 80%, and no variation at higher loadings. The dominant role of the guest-induced pressure over the framework, at higher loadings, is evident from the figure, as the strings tend to expand as much as possible. Deviations from 1.0 are caused by thermal noise. At lower loadings, the collisions of these molecules with the framework are not enough to keep the strings extended. The most relevant effects are, instead, the flexibility of the rods junctions and the internal deformations of the rods. The collisions play a key role in deforming the lines, as can be inferred by the rise of the line deformation parameter with an increase of temperature (Figure 4c). The ZTE behavior (curves at ca. 60% loadings) is then the result of the compensating effect between the increase of the atomic line deformation, that is, the relatively smaller geometric line length and the natural increase of the length of the bonds.

The central and bottom panels of Figure 5 show the relative size of the oxocluster and BDC with respect to the cell size. The behavior of the oxocluster unit shows a monotonous variation with temperature, and it is mostly independent of loading, for the three molecules. However, we observed that the effects of loading on the shape and size of the BDC unit are radically different. At low loadings, the relative distortion of the BDC unit increases with the increase of temperature, and at high loadings, the relative distortion decreases. This is related to the ability of the BDC unit to be distorted. This observation is further supported by the analysis of the angle formed by the medium points of the oxygen atoms in the carboxylic groups and the carbon atoms in the benzene ring (top panel Figure S7).

One important conclusion arisen from the structural analysis, in connection to the TE, is related to the flexibility of MOFs, particularly to the flexibility and deformations of both, the junctions between molecular units, and the units themselves. There is an accepted understanding that flexibility in MOFs can be depicted in a mechanical view based on the flexibility of the junctions connecting rigid units.[62] However, this mechanical approach fails to explain the flexibility behavior for the isostructural MOFs MIL-47 and MIL-53, being the first rigid and the second flexible.[63] Our results indicate, moreover, that besides the primary source of flexibility associated with the junction units, the nature of the units, is also essential, and the deformations inside the units also contribute to the overall flexibility of the materials. A detailed description of the intra- and interunit deformations, in terms of relevant angles, distances, and distortions parameters, can be found in the Supporting Information, Figures S5−S8.

In our investigation of routes to control thermal expansion, we have shown that there is a clear connection between adsorbate loading, local and long-range distortions, and thermo-structural behavior. We have shown that the material can be regarded as assembled by relatively rigid units, such as the oxoclusters and benzene rings, and by units with some degree of flexibility, such as the fragments composed by the acid groups with the connecting carbon atom from the benzene ring, and flexible junctions. By focusing on the strings of atoms (Figure 4d), a large number of degrees of freedom can be associated with this particular structural motif, although their motions are constrained by the 3-D architecture of the network. In addition, the internal motion of each grid is restricted by the presence of atomic rings and clusters. The NTE thermal behavior of the empty framework can then be easily interpreted in terms of the rigid unit modes (RUM) formalism,[56,64] which supports the presence of cooperative modes. They generate disorder, which makes the atomic string to deviate more from the ideal line as temperature increases, as can be observed in Figure 5, bottom. In the presence of adsorbates, host−guest attraction causes a degree of coordination between the movement of the adsorbate molecules and the flexible constituents of the material. This explains the observed behavior. At low loading, the adsorbate molecules have large local mobility, which therefore increases the NTE coefficients. At high loading, the average position of the center of mass of the adsorbate molecules is rather static, due to the lack of available space, which consequently rules out the appearance of the cooperative modes responsible of NTE. In the latter case, the close intermolecular distances provoke rocking motions that result in PTE.

On this basis, it is easy to rationalize why, at low loading, the qualitative behavior of the thermal expansion is similar for a wide range of temperatures. We observe that guest molecules are localized around certain positions and have negligible impact on the host−host interactions that are associated with the NTE regime. Conversely, at high loading, there are "steric shielding effects" on the thermal expansion behavior, that is, host−host interactions are seemingly weakened by the large number of guest molecules.

DOI: 10.1021/acs.chemmater.6b03457
Chem. Mater. 2016, 28, 8296−8304

From a materials design point of view, we know that long-range, Coulombic interactions can finely modulate the intrinsic TE properties of a MOF.[65] It is known that the charge distribution in a MOF can be tailored by changing the chemical composition.[66−70] For example, in a combined experimental and computational work, it was shown that varying the nature of the metal in the MOFs M_2(m-dobdc) (M = Mg, Mn, Fe, Co, Ni; m-dobdc4− = 4,6-dioxido-1,3-benzenedicarboxylate), the polarity is systematically changed.[66] On the other hand, we show here that, despite the colligative behavior found for the thermostructural properties, the nature of the molecules influences the change of the cell volume at given loadings. Overall, we advance that by exploiting the modulation of TE given by long-range, Coulombic interactions, in connection with the guest-assisted control shown in this work, it is possible to achieve a large versatility in controlling the thermal expansion characteristics of the material.

CONCLUSIONS

In summary, we devised an approach with which it is possible to create systems with fine-tuned thermal expansion coefficients thanks to the structural properties of MOFs. We found a complex interplay between competing effects, which permits the control of the thermal expansion. The attractive host−guest interactions induce the cell to contract, particularly at low loading. In these conditions, upon an increase of temperature, the thermal disorder increases, and thus, the coupled host−guest movements largely distort the atomic strings, which reduce the cell parameters, expressed as NTE. With increasing loading, the collisions of the guest molecules to the framework tend to direct the atomic strings to straight lines and therefore induce an increase of the cell parameter. At about 60% of loading, this effect is not enough yet to produce PTE, which, combined with the natural increase of bond distances, results in ZTE. At higher loadings, the increasing number of collisions leads to significant effects on the framework dynamics, much larger than the volume-reducing effect of the attractive host−guest interactions, so PTE is observed. In summary, we have found a surprising colligative behavior of the system, which determines the thermal expansion of MOF-5, featured by a general behavior that, for these similarly sizes molecules, is not particularly dependent on the nature of the adsorbed molecule.

ASSOCIATED CONTENT

Supporting Information

The Supporting Information is available free of charge on the ACS Publications website at DOI: 10.1021/acs.chemmater.6b03457.

Snapshots of MOF-5 saturated with adsorbed molecules; figures and tables with relevant geometrical and structural parameters (PDF)

AUTHOR INFORMATION

Corresponding Authors

*E-mail: rruisal@upo.es.
*E-mail: D.Dubbeldam@uva.nl
*E-mail: scalero@upo.es.

Author Contributions

The manuscript was written through contributions of all authors.

Notes

The authors declare no competing financial interest.

ACKNOWLEDGMENTS

The research leading to these results has received funding from the European Research Council under the European Union's Seventh Framework Programme (FP7/2007-2013)/(ERC Grant Agreement No. [279520]), the Spanish "Ministerio de Economía y Competitividad" (CTQ2013-48396-P), and The Netherlands Council for Chemical Sciences (NWO/CW) through a VIDI grant. S.R.G.B. thanks the "Ministerio de Economía y Competitividad" for his predoctoral fellowship. This work made use of the computer services provided by the high performance computer center Alhambra (at the University of Granada).

REFERENCES

(1) Han, B.; M, C.; Park, S.; Li, L.; Verma, K. Effect of Substrate CTE on Solder Ball Reliability of Flip Chip PBGA Package Assembly. *J. Surf. Mount Technol.* **1996**, 43−52.
(2) Darolia, R. Thermal Barrier Coatings Technology: Critical Review, Progress Update, Remaining Challenges and Prospects. *Int. Mater. Rev.* **2013**, *58*, 315−348.
(3) Della Gaspera, E.; Tucker, R.; Star, K.; Lan, E. H.; Ju, Y. S.; Dunn, B. Copper-Based Conductive Composites with Tailored Thermal Expansion. *ACS Appl. Mater. Interfaces* **2013**, *5*, 10966−10974.
(4) Hu, B.; Zhang, Y.; Chen, W.; Xu, C.; Wang, Z. L. Self-heating and External Strain Coupling Induced Phase Transition of VO2 Nanobeam as Single Domain Switch. *Adv. Mater.* **2011**, *23*, 3536−3541.
(5) Kelly, A.; Stearn, R. J.; McCartney, L. N. Composite Materials of Controlled Thermal Expansion. *Compos. Sci. Technol.* **2006**, *66*, 154−159.
(6) Tallentire, S. E.; Child, F.; Fall, I.; Vella-Zarb, L.; Evans, I. R.; Tucker, M. G.; Keen, D. A.; Wilson, C.; Evans, J. S. O. Systematic and Controllable Negative, Zero, and Positive Thermal Expansion in Cubic Zr1−xSnxMo2O8. *J. Am. Chem. Soc.* **2013**, *135*, 12849−12856.
(7) Banks-Sills, L. 50th Anniversary Article: Review on Interface Fracture and Delamination of Composites. *Strain* **2014**, *50*, 98−110.
(8) Sethi, S.; Ray, B. C. Environmental Effects on Fibre Reinforced Polymeric Composites: Evolving Reasons and Remarks on Interfacial Strength and Stability. *Adv. Colloid Interface Sci.* **2015**, *217*, 43−67.
(9) Mary, T. A.; Evans, J. S. O.; Vogt, T.; Sleight, A. W. Negative Thermal Expansion from 0.3 to 1050 K in ZrW_2O_8. *Science* **1996**, *272*, 90.
(10) Carey, T.; Tang, C. C.; Hriljac, J. A.; Anderson, P. A. Chemical Control of Thermal Expansion in Cation-Exchanged Zeolite A. *Chem. Mater.* **2014**, *26*, 1561−1566.
(11) Collings, I. E.; Tucker, M. G.; Keen, D. A.; Goodwin, A. L. Geometric Switching of Linear to Area Negative Thermal Expansion in Uniaxial Metal-Organic Frameworks. *CrystEngComm* **2014**, *16*, 3498−3506.
(12) Lock, N.; Christensen, M.; Kepert, C. J.; Iversen, B. B. Effect of Gas Pressure on Negative Thermal Expansion in MOF-5. *Chem. Commun.* **2013**, *49*, 789−791.
(13) Peterson, V. K.; Kearley, G. J.; Wu, Y.; Ramirez-Cuesta, A. J.; Kemner, E.; Kepert, C. J. Local Vibrational Mechanism for Negative Thermal Expansion: A Combined Neutron Scattering and First-Principles Study. *Angew. Chem., Int. Ed.* **2010**, *49*, 585−588.
(14) Yot, P. G.; Boudene, Z.; Macia, J.; Granier, D.; Vanduyfhuys, L.; Verstraelen, T.; Van Speybroeck, V.; Devic, T.; Serre, C.; Ferey, G.; Stock, N.; Maurin, G. Metal-Organic Frameworks as Potential Shock Absorbers: the Case of the Highly Flexible MIL-53(Al). *Chem. Commun.* **2014**, *50*, 9462−9464.
(15) Li, W.; Henke, S.; Cheetham, A. K. Research Update: Mechanical Properties of Metal-Organic Frameworks − Influence of Structure and Chemical Bonding. *APL Mater.* **2014**, *2*, 123902.
(16) Dubbeldam, D.; Walton, K. S.; Ellis, D. E.; Snurr, R. Q. Exceptional Negative Thermal Expansion in Isoreticular Metal−Organic Frameworks. *Angew. Chem., Int. Ed.* **2007**, *46*, 4496−4499.

DOI: 10.1021/acs.chemmater.6b03457
Chem. Mater. 2016, 28, 8296−8304

(17) Rowsell, J. L. C.; Spencer, E. C.; Eckert, J.; Howard, J. A. K.; Yaghi, O. M. Gas Adsorption Sites in a Large-Pore Metal-Organic Framework. *Science* **2005**, *309*, 1350−1354.
(18) Zhou, W.; Wu, H.; Yildirim, T.; Simpson, J. R.; Walker, A. R. H. Origin of the Exceptional Negative Thermal Expansion in Metal-Organic Framework-5 Zn4O(1,4−benzenedicarboxylate)3. *Phys. Rev. B: Condens. Matter Mater. Phys.* **2008**, *78*, 054114.
(19) Yang, C.; Wang, X.; Omary, M. A. Crystallographic Observation of Dynamic Gas Adsorption Sites and Thermal Expansion in a Breathable Fluorous Metal−Organic Framework. *Angew. Chem., Int. Ed.* **2009**, *48*, 2500−2505.
(20) Joo, J.; Kim, H.; Han, S. S. Volume Shrinkage of a Metal-Organic Framework Host Induced by the Dispersive Attraction of Guest Gas Molecules. *Phys. Chem. Chem. Phys.* **2013**, *15*, 18822−18826.
(21) Boutin, A.; Coudert, F.-X.; Springuel-Huet, M.-A.; Neimark, A. V.; Férey, G.; Fuchs, A. H. The Behavior of Flexible MIL-53(Al) upon CH4 and CO2 Adsorption. *J. Phys. Chem. C* **2010**, *114*, 22237−22244.
(22) Neimark, A. V.; Coudert, F.-X.; Triguero, C.; Boutin, A.; Fuchs, A. H.; Beurroies, I.; Denoyel, R. Structural Transitions in MIL-53 (Cr): View from Outside and Inside. *Langmuir* **2011**, *27*, 4734−4741.
(23) Grobler, I.; Smith, V. J.; Bhatt, P. M.; Herbert, S. A.; Barbour, L. J. Tunable Anisotropic Thermal Expansion of a Porous Zinc(II) Metal−Organic Framework. *J. Am. Chem. Soc.* **2013**, *135*, 6411−6414.
(24) Serre, C.; Millange, F.; Thouvenot, C.; Noguès, M.; Marsolier, G.; Louër, D.; Férey, G. Very Large Breathing Effect in the First Nanoporous Chromium(III)-Based Solids: MIL-53 or CrIII(OH)·{O2C−C6H4−CO2}·{HO2C−C6H4−CO2H}x·H2Oy. *J. Am. Chem. Soc.* **2002**, *124*, 13519−13526.
(25) Matsuda, R.; Kitaura, R.; Kitagawa, S.; Kubota, Y.; Kobayashi, T. C.; Horike, S.; Takata, M. Guest Shape-Responsive Fitting of Porous Coordination Polymer with Shrinkable Framework. *J. Am. Chem. Soc.* **2004**, *126*, 14063−14070.
(26) Yaghi, O. M.; Eddaoudi, M.; O'Keeffe, M.; Li, H. Design and Synthesis of an Exceptionally Stable and Highly Porous Metal-Organic Framework. *Nature* **1999**, *402*, 276−279.
(27) Bellarosa, L.; Castillo, J. M.; Vlugt, T.; Calero, S.; López, N. On the Mechanism Behind the Instability of Isoreticular Metal−Organic Frameworks (IRMOFs) in Humid Environments. *Chem. - Eur. J.* **2012**, *18*, 12260−12266.
(28) Sarmiento-Perez, R. A.; Rodriguez-Albelo, L. M.; Gomez, A.; Autie-Perez, M.; Lewis, D. W.; Ruiz-Salvador, A. R. Surprising Role of the BDC Organic Ligand in the Adsorption of CO2 by MOF-5. *Microporous Mesoporous Mater.* **2012**, *163*, 186−191.
(29) Guo, H.-c.; Shi, F.; Ma, Z.-f.; Liu, X.-q. Molecular Simulation for Adsorption and Separation of CH4/H2 in Zeolitic Imidazolate Frameworks. *J. Phys. Chem. C* **2010**, *114*, 12158−12165.
(30) Ray, K. G.; Olmsted, D.; He, N.; Houndonougbo, Y.; Laird, B. B.; Asta, M. van der Waals Density Functional Study of CO2 Binding in Zeolitic Imidazolate Frameworks. *Phys. Rev. B: Condens. Matter Mater. Phys.* **2012**, *85*, 085410.
(31) Andirova, D.; Cogswell, C. F.; Lei, Y.; Choi, S. Effect of the Structural Constituents of Metal Organic Frameworks on Carbon Dioxide Capture. *Microporous Mesoporous Mater.* **2016**, *219*, 276−305.
(32) He, W.-W.; Yang, G.-S.; Tang, Y.-J.; Li, S.-L.; Zhang, S.-R.; Su, Z.-M.; Lan, Y.-Q. Phenyl Groups Result in the Highest Benzene Storage and Most Efficient Desulfurization in a Series of Isostructural Metal−Organic Frameworks. *Chem. - Eur. J.* **2015**, *21*, 9784−9789.
(33) Hu, Y. H.; Zhang, L. Amorphization of Metal-Organic Framework MOF-5 at Unusually Low Applied Pressure. *Phys. Rev. B: Condens. Matter Mater. Phys.* **2010**, *81*, 174103.
(34) Ma, L.; Jin, A.; Xie, Z.; Lin, W. Freeze Drying Significantly Increases Permanent Porosity and Hydrogen Uptake in 4,4-Connected Metal−Organic Frameworks. *Angew. Chem., Int. Ed.* **2009**, *48*, 9905−9908.
(35) Bennett, T. D.; Sotelo, J.; Tan, J.-C.; Moggach, S. A. Mechanical Properties of Zeolitic Metal-Organic Frameworks: Mechanically Flexible Topologies and Stabilization Against Structural Collapse. *CrystEngComm* **2015**, *17*, 286−289.
(36) Khutia, A.; Rammelberg, H. U.; Schmidt, T.; Henninger, S.; Janiak, C. Water Sorption Cycle Measurements on Functionalized MIL-101Cr for Heat Transformation Application. *Chem. Mater.* **2013**, *25*, 790−798.
(37) Begum, S.; Horike, S.; Kitagawa, S.; Krautscheid, H. Water Stable Triazolyl Phosphonate MOFs: Steep Water Uptake and Facile Regeneration. *Dalton Trans.* **2015**, *44*, 18727−18730.
(38) Mondloch, J. E.; Katz, M. J.; Planas, N.; Semrouni, D.; Gagliardi, L.; Hupp, J. T.; Farha, O. K. Are Zr6-Based MOFs Water Stable? Linker Hydrolysis vs. Capillary-Force-Driven Channel Collapse. *Chem. Commun.* **2014**, *50*, 8944−8946.
(39) Dubbeldam, D.; Calero, S.; Ellis, D. E.; Snurr, R. Q. RASPA: Molecular Simulation Software for Adsorption and Diffusion in Flexible Nanoporous Materials. *Mol. Simul.* **2016**, *42*, 81−101.
(40) Widom, B. Some Topics in the Theory of Fluids. *J. Chem. Phys.* **1963**, *39*, 2808−2812.
(41) Rappe, A. K.; Casewit, C. J.; Colwell, K. S.; Goddard, W. A.; Skiff, W. M. UFF, a Full Periodic-Table Force-Field for Molecular Mechanics and Molecular-Dynamics Simulations. *J. Am. Chem. Soc.* **1992**, *114*, 10024−10035.
(42) Jorgensen, W. L.; Tirado-Rives, J. The OPLS [Optimized Potentials for Liquid Simulations] Potential Functions for Proteins, Energy Minimizations for Crystals of Cyclic Peptides and Crambin. *J. Am. Chem. Soc.* **1988**, *110*, 1657−1666.
(43) Jorgensen, W. L.; Maxwell, D. S.; Tirado-Rives, J. Development and Testing of the OPLS All-Atom Force Field on Conformational Energetics and Properties of Organic Liquids. *J. Am. Chem. Soc.* **1996**, *118*, 11225−11236.
(44) Ewald, P. P. Die Berechnung optischer und elektrostatischer Gitterpotentiale. *Ann. Phys.* **1921**, *369*, 253−287.
(45) Tosi, M. P. Cohesion of Ionic Solids in the Born Model. *Solid State Phys.* **1964**, *16*, 1.
(46) Jorgensen, W. L.; Laird, E. R.; Nguyen, T. B.; Tirado-Rives, J. Monte Carlo simulations of pure liquid substituted benzenes with OPLS potential functions. *J. Comput. Chem.* **1993**, *14*, 206−215.
(47) Nemkevich, A.; Burgi, H.-B.; Spackman, M. A.; Corry, B. Molecular dynamics simulations of structure and dynamics of organic molecular crystals. *Phys. Chem. Chem. Phys.* **2010**, *12*, 14916−14929.
(48) Caleman, C.; van Maaren, P. J.; Hong, M.; Hub, J. S.; Costa, L. T.; van der Spoel, D. Force Field Benchmark of Organic Liquids: Density, Enthalpy of Vaporization, Heat Capacities, Surface Tension, Isothermal Compressibility, Volumetric Expansion Coefficient, and Dielectric Constant. *J. Chem. Theory Comput.* **2012**, *8*, 61−74.
(49) Frenkel, D.; Smit, B. *Understanding Molecular Simulation*; Academic Press: San Diego, CA, 1996.
(50) Martyna, G. J.; Tuckerman, M. E.; Tobias, D. J.; Klein, M. L. Explicit Reversible Integrators for Extended Systems Dynamics. *Mol. Phys.* **1996**, *87*, 1117−1157.
(51) Tuckerman, M. E.; Alejandre, J.; Lopez-Rendon, R.; Jochim, A. L.; Martyna, G. J. A Liouville-Operator Derived Measure-Preserving Integrator for Molecular Dynamics Simulations in the Isothermal−Isobaric Ensemble. *J. Phys. A: Math. Gen.* **2006**, *39*, 5629.
(52) Eddaoudi, M.; Li, H.; Yaghi, O. M. Highly Porous and Stable Metal−Organic Frameworks: Structure Design and Sorption Properties. *J. Am. Chem. Soc.* **2000**, *122*, 1391−1397.
(53) Shim, W.-G.; Hwang, K.-J.; Chung, J.-T.; Baek, Y.-S.; Yoo, S.-J.; Kim, S.-C.; Moon, H.; Lee, J.-W. Adsorption and thermodesorption characteristics of benzene in nanoporous metal organic framework MOF-5. *Adv. Powder Technol.* **2012**, *23*, 615−619.
(54) Eddaoudi, M.; Kim, J.; Rosi, N.; Vodak, D.; Wachter, J.; O'Keeffe, M.; Yaghi, O. M. Systematic Design of Pore Size and Functionality in Isoreticular MOFs and their Application in Methane Storage. *Science* **2002**, *295*, 469−472.
(55) Welche, P. R. L.; Heine, V.; Dove, M. T. Negative Thermal Expansion in Beta-Quartz. *Phys. Chem. Miner.* **1998**, *26*, 63−77.
(56) Pryde, A. K. A.; Hammonds, K. D.; Dove, M. T.; Heine, V.; Gale, J. D.; Warren, M. C. Origin of the Negative Thermal Expansion in ZrW2O8 and ZrV2O7. *J. Phys.: Condens. Matter* **1996**, *8*, 10973.

DOI: 10.1021/acs.chemmater.6b03457
Chem. Mater. 2016, 28, 8296−8304

(57) Barrera, G. D.; Bruno, J. A. O.; Barron, T. H. K.; Allan, N. L. Negative Thermal Expansion. *J. Phys.: Condens. Matter* **2005**, *17*, R217.
(58) Lock, N.; Christensen, M.; Wu, Y.; Peterson, V. K.; Thomsen, M. K.; Piltz, R. O.; Ramirez-Cuesta, A. J.; McIntyre, G. J.; Noren, K.; Kutteh, R.; Kepert, C. J.; Kearley, G. J.; Iversen, B. B. Scrutinizing Negative Thermal Expansion in MOF-5 by Scattering Techniques and AB-Initio Calculations. *Dalton Trans.* **2013**, *42*, 1996−2007.
(59) Lock, N.; Wu, Y.; Christensen, M.; Cameron, L. J.; Peterson, V. K.; Bridgeman, A. J.; Kepert, C. J.; Iversen, B. B. Elucidating Negative Thermal Expansion in MOF-5. *J. Phys. Chem. C* **2010**, *114*, 16181−16186.
(60) Fang, H.; Dove, M. T.; Phillips, A. E. Common Origin of Negative Thermal Expansion and other Exotic Properties in Ceramic and Hybrid Materials. *Phys. Rev. B: Condens. Matter Mater. Phys.* **2014**, *89*, 214103.
(61) Balestra, S. R. G.; Hamad, S.; Ruiz-Salvador, A. R.; Domínguez-García, V.; Merkling, P. J.; Dubbeldam, D.; Calero, S. Understanding Nanopore Window Distortions in the Reversible Molecular Valve Zeolite RHO. *Chem. Mater.* **2015**, *27*, 5657−5667.
(62) Sarkisov, L.; Martin, R. L.; Haranczyk, M.; Smit, B. On the Flexibility of Metal−Organic Frameworks. *J. Am. Chem. Soc.* **2014**, *136*, 2228−2231.
(63) Devautour-Vinot, S.; Maurin, G.; Henn, F.; Serre, C.; Devic, T.; Ferey, G. Estimation of the Breathing Energy of Flexible MOFs by Combining TGA and DSC techniques. *Chem. Commun.* **2009**, 2733−2735.
(64) Hammonds, K. D.; Heine, V.; Dove, M. T. Insights Into Zeolite Behaviour from the Rigid Unit Mode Model. *Phase Transitions* **1997**, *61*, 155−172.
(65) Hamad, S.; Balestra, S. R. G.; Bueno-Perez, R.; Calero, S.; Ruiz-Salvador, A. R. Atomic Charges for Modeling Metal−Organic Frameworks: Why and How. *J. Solid State Chem.* **2015**, *223*, 144−151.
(66) Kapelewski, M. T.; Geier, S. J.; Hudson, M. R.; Stück, D.; Mason, J. A.; Nelson, J. N.; Xiao, D. J.; Hulvey, Z.; Gilmour, E.; FitzGerald, S. A.; Head-Gordon, M.; Brown, C. M.; Long, J. R. M2(m-dobdc) (M = Mg, Mn, Fe, Co, Ni) Metal−Organic Frameworks Exhibiting Increased Charge Density and Enhanced H2 Binding at the Open Metal Sites. *J. Am. Chem. Soc.* **2014**, *136*, 12119−12129.
(67) Gygi, D.; Bloch, E. D.; Mason, J. A.; Hudson, M. R.; Gonzalez, M. I.; Siegelman, R. L.; Darwish, T. A.; Queen, W. L.; Brown, C. M.; Long, J. R. Hydrogen Storage in the Expanded Pore Metal−Organic Frameworks M2(dobpdc) (M = Mg, Mn, Fe, Co, Ni, Zn). *Chem. Mater.* **2016**, *28*, 1128−1138.
(68) Pham, T.; Forrest, K. A.; Banerjee, R.; Orcajo, G.; Eckert, J.; Space, B. Understanding the H2 Sorption Trends in the M-MOF-74 Series (M = Mg, Ni, Co, Zn). *J. Phys. Chem. C* **2015**, *119*, 1078−1090.
(69) Rosnes, M. H.; Opitz, M.; Frontzek, M.; Lohstroh, W.; Embs, J. P.; Georgiev, P. A.; Dietzel, P. D. C. Intriguing Differences in Hydrogen Adsorption in CPO-27 Materials Induced by Metal Substitution. *J. Mater. Chem. A* **2015**, *3*, 4827−4839.
(70) Pham, T.; Forrest, K. A.; Eckert, J.; Space, B. Dramatic Effect of the Electrostatic Parameters on H2 Sorption in an M-MOF-74 Analogue. *Cryst. Growth Des.* **2016**, *16*, 867−874.

DOI: 10.1021/acs.chemmater.6b03457
Chem. Mater. 2016, 28, 8296−8304